Formation of Surface-Bound Acyl Groups by Reaction of Acyl Halides on Ge(100)−2×1

Michael A. Filler, Albert J. Keung, David W. Porter, and Stacey F. Bent*

Department of Chemical Engineering, Stanford University, Stanford, California 94305

Received: October 5, 2005; In Final Form: January 3, 2006

We have investigated the reaction of a series of acyl halides, including acetyl chloride, acetyl bromide, acetyl-d_3 chloride, benzoyl chloride, and pivaloyl chloride, on Ge(100)−2×1 with multiple internal reflection infrared (MIR-IR) spectroscopy, X-ray photoelectron spectroscopy (XPS), and density functional theory (DFT). Infrared spectra following saturation exposures of acetyl chloride and acetyl bromide to Ge(100)−2×1 at 310 K are nearly identical, both exhibiting strong ν(C═O) stretching peaks near 1685 cm^{-1} and no vibrational modes in the ν(Ge−H) region. These data provide strong evidence for the presence of a surface-bound acetyl group on Ge(100)−2×1, which results from a C−X dissociation reaction (where X = Cl, Br). For acetyl chloride, DFT calculations predict that the barrier to C−Cl dissociation is only 1 kcal/mol above a chlorine-bound precursor state and is considerably smaller than barriers leading to the [2+2] C═O cycloaddition and α-CH dissociation products. In addition to the C−X dissociation product, both infrared and photoelectron results point to the presence of a second structure for acetyl halides where the oxygen of the surface-bound acetyl group donates charge to a nearby surface atom. This interaction is not observed for benzoyl chloride and pivaloyl chloride.

I. Introduction

As the limits of traditional device scaling become increasingly apparent, there is considerable interest in the combination of organic and inorganic materials. It is believed that the current knowledge base for microelectronics fabrication combined with the tailorability of organic materials and the precise interface control afforded by atomically clean surfaces may lead to novel applications in molecular electronics[1−4] and chemical sensing.[5] Therefore, the covalent attachment of organic molecules to the (100)−2×1 reconstructed, group IV semiconductor surfaces of silicon and germanium has received considerable attention in recent years.[6−10]

It is expected that many of these future applications will require the precisely-controlled, well-ordered growth of ultrathin organic films. While solution-based techniques with hydrogen-terminated surfaces enable the selective attachment of bifunctional precursors with various functionalities at the semiconductor interface,[11−15] most of the vacuum-based reactions examined to date on clean group IV (100)−2×1 semiconductor surfaces exhibit shortcomings both in the degree of selectivity toward a single product and in the degree of order in the organic layer.[16−19] However, proper control of the kinetics of competing reaction pathways may be a useful method with which to combat this problem and selectively attach a nonsymmetric bifunctional or multifunctional molecule to Si(100)−2×1 or Ge(100)−2×1. Many theoretical studies predict that the activation barriers for the reaction of various organic functional groups on Si(100)−2×1 and Ge(100)−2×1 can differ by 10−15 kcal/mol or more,[9,16,20,21] leading to approximately a 10^7−10^{10} times difference in the rate of reaction. Therefore, it seems likely that sufficient molecular engineering of a multifunctional compound could result in a near 100% selectively attached organic monolayer. Retention of at least one reactive moiety following adsorption would also open the door to the layer-by-layer deposition of tailored, organic, ultrathin films under vacuum conditions similar to those reported by Bitzer et al.[22] and Kim et al.[23] This type of molecular layer deposition is analogous to the atomic layer deposition (ALD) of high-κ dielectric films,[24] and can be binary, ternary, or other combinations of multifunctional organic molecules reacted in a sequential fashion.

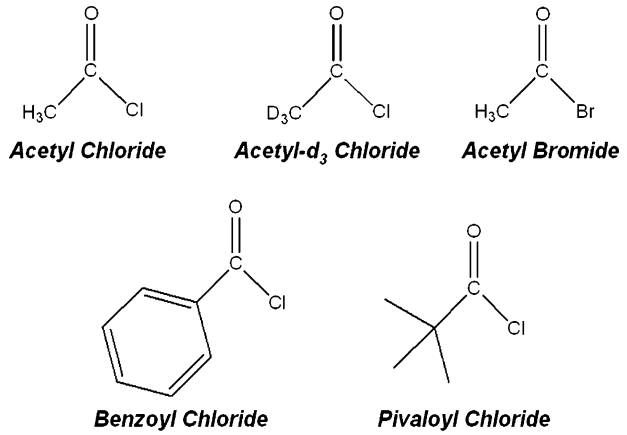

Figure 1. Acyl halide probe molecules investigated in this study.

To this end, we selected a series of acyl halides, shown in Figure 1, as model molecules to examine the possibility of achieving a highly selective surface product distribution. Acyl halides are highly susceptible to nucleophilic attack at the carbonyl carbon, which often leads to cleavage of the C−X bond (where X denotes a halogen atom). For example, the nucleophilic attack of acetyl halides by ammonia or methanol leads to the formation of acetamide and methyl acetate, respectively.[25] While halides are considered excellent leaving groups in the solution phase, as a result of their ability to be easily solvated, one must be careful when making similar analogies under vacuum conditions.

In a manner similar to the attack of acyl halides in solution by nucleophiles, the nucleophilic Ge dimer atom could attack

* Address correspondence to this author. E-mail: sbent@stanford.edu.

10.1021/jp055685+ CCC: $33.50
Published on Web 02/08/2006

the carbonyl carbon. Hamers and co-workers observed a similar attack by the nucleophilic dimer atom during the coadsorption of trimethylamine and boron trifluoride on Si(100)−2×1.[26] In the present case, this type of reaction may cause the halogen atom to dissociate and bond to the electrophilic dimer atom to give a C−X dissociated product. On the basis of previous investigations of ketones and aldehydes on Si(100)−2×1 and Ge(100)−2×1,[27,28] it is also plausible that acyl halides could form [2+2] C═O cycloaddition or α-CH dissociation surface adducts after passing through an oxygen dative-bonded precursor state.

Experimental data from this study indicate that C−X dissociation dominates over other pathways. In addition, interactions with nearby surface sites may play a significant role in the reaction of acetyl halides on Ge(100)−2×1. While single dimer models are known to work well for some systems,[21,29,30] recently published results add to a mounting body of evidence that, even for simple molecules such as ethylene,[31] maleic anhydride,[32] pyrimidine,[33] acrylonitrile,[34] and cyclohexadiene,[19] products regularly form between multiple surface dimers on Si(100)−2×1 and Ge(100)−2×1. Therefore, a full understanding of the surface chemistry often requires the consideration of interactions between the adsorbate and multiple surface dimers.

II. Experimental and Computational Details

All experiments were completed under ultrahigh vacuum conditions (UHV) in two different reaction chambers described previously.[21,35] For X-ray photoelectron spectroscopy experiments, the Ge(100) crystal (0.1−0.39 Ω·cm, p-type, B-doped) was cleaned by Ar^+ sputtering at 900 K (20 mA emission current, 1.0 keV accelerating voltage, 12 μA sample current) for 30 min followed by annealing to 1000 K for 15 min. Following several sputtering/annealing cycles, carbon, oxygen, and nitrogen levels were below the detection limit of our X-ray spectrometer, and STM images confirmed a mixed c(4×2) and 2×1 surface reconstruction.[36] Due to interference by the germanium Auger series, it was necessary to record C(1s) and O(1s) photoelectron spectra (250 W = 12.5 kV anode voltage, 20 mA emission current) with the Al and Mg anodes, respectively. A Ge(3s) plasmon near 200 eV and a Ge(LMM) Auger satellite near 270 eV prevent the quantitative analysis of the Cl(2p) and Cl(2s) photoelectron peaks, respectively. The emitted electrons were collected at a takeoff angle of 25°, an acceptance angle of ca. ±5°, and a pass energy of 25 eV. The Ge(3d) photoelectron peak was employed as an internal standard with which to calibrate the energy scale and peak intensity. Shirley baseline subtractions[37] were applied, and a chemically realistic number of Voigt components were fit to each photoelectron spectrum. With our spectrometer set at a pass energy of 25 eV, the C(1s) spectrum of ethylene chemisorbed on Ge(100)−2×1 shows a single peak centered at 283.7 eV with a fwhm of 1.6 eV, while the O(1s) spectrum of methanol on Ge(100)−2×1 reveals a peak at 531.2 eV with a fwhm of nearly 2.0 eV. While all synthetic components within each spectrum were forced to have the same fwhm, the value was allowed to be 1.6 ± 0.2 and 2.0 ± 0.2 eV for the C(1s) and O(1s) photoelectron spectra, respectively.

For infrared experiments, the Ge(100) crystal was prepared by Ar^+ sputtering at room temperature (20 mA emission current, 0.5 keV accelerating voltage, 7−8 μA sample current) for 20 min followed by annealing to 900 K for 5 min. Although the cleaning procedure for infrared experiments differed from that for XPS experiments, after several sputtering/annealing cycles, the LEED pattern of the 2×1 surface reconstruction was clearly visible. Auger electron spectroscopy (AES) verified that carbon, oxygen, and nitrogen surface concentrations were undetectable. Infrared spectra were collected in a multiple internal reflection (MIR) geometry by employing a BioRad FTS-60A Fourier transform infrared (FTIR) spectrometer equipped with a liquid nitrogen cooled narrow-band mercury−cadmium−telluride (MCT) detector. To record infrared spectra of the unreacted molecules, several multilayers were condensed on the sample surface at low temperature. While surface adduct identification would be greatly facilitated by the analysis of various alkane and alkene ν(C−H) stretching modes near 3000 cm^{-1}, the weakness of the infrared absorption in this region for the acyl halides in this study forces us to rely on modes with absorption energies in the fingerprint region of the infrared spectrum. All spectra were corrected for baseline sloping.

Acetyl chloride (Aldrich, 99+%), acetyl bromide (Aldrich, 99%), acetyl chloride-d_3 (Aldrich, 99+ atom D %), pivaloyl chloride (Aldrich, 99%), and benzoyl chloride (Aldrich, 99%) are clear liquids under ambient conditions, and transfer to sample vials was completed under dry air purge. Each compound was purified by several freeze−pump−thaw cycles before exposure to the crystal surface through a variable leak valve. Surface exposures are reported in Langmuirs (1 L = 10^{-6} Torr·s) and pressures were not corrected for ionization gauge sensitivity. In an attempt to minimize reaction of these highly corrosive compounds with the inner walls of the stainless steel gas handling manifold, the compounds were allowed to enter the vacuum chambers within 5 s of filling the lines. Following each surface exposure, the manifold lines were pumped out to less than 20 mTorr before refilling for the following dose. An in situ quadrupole mass spectrometer confirmed the molecular identity and purity of each compound after introduction to either chamber.

Electronic structure calculations were completed with the Gaussian 98 software package,[38] using Becke3 Lee−Yang−Parr (B3LYP) three-parameter density functional theory.[39] The B3LYP functional is composed of the Lee−Yang−Parr and VWN correlation functionals[40,41] in addition to the Becke hybrid gradient-corrected exchange functional.[42] Previous studies of B3LYP indicate that it provides predictive results for similar systems[9,16,17,21] and is in good agreement when experimental results are available.[21,43] Geometries of important local minima and transition states on the potential energy surface were calculated with the polarized double-ζ, 6-31G(d) basis set without geometrical constraints followed by a single point calculation at the 6-31G(d) geometry with the more accurate, triple-ζ, 6-311++G(2df,pd) basis set. Local minima and transition states were verified with frequency calculations of the optimized structure with the 6-31G(d) basis set. The reported energies were not zero-point corrected.

Due to the predominantly localized bonding of group IV (100)−2×1 semiconductor surfaces, we modeled the Ge(100)−2×1 surface as a dimer cluster. Most frequently, Si(100)−2×1 is modeled with a Si_9H_{12} cluster where the top two Si atoms compose the surface dimer. The remaining seven Si atoms compose three subsurface layers which are hydrogen terminated to preserve the sp^3 hybridization of the bulk diamond lattice. In this study, the Ge surface is modeled as a $Ge_2Si_7H_{12}$ cluster, where the two dimer atoms are replaced with Ge. Calculations at the B3LYP/6-311++G(2df,pd) level of theory for 1,3-butadiene cycloaddition products on a $Ge_2Si_7H_{12}$ cluster result in a binding energy within 1−2 kcal/mol of that found with the Ge_9H_{12} cluster.[44] In the present work, DFT is used to predict

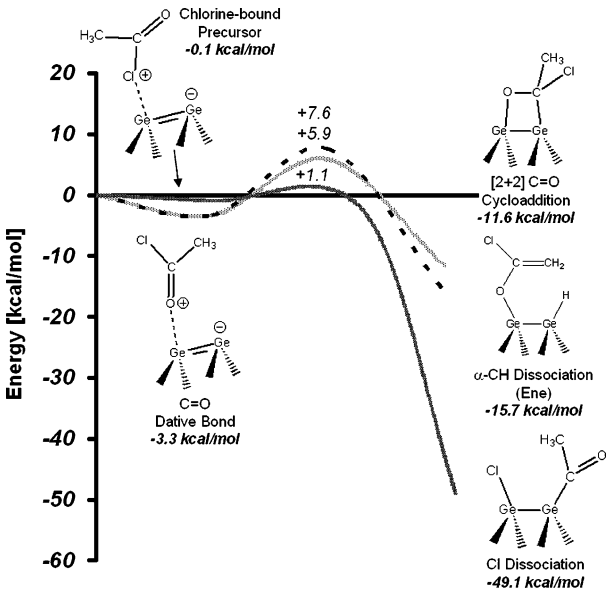

Figure 2. Critical points on the calculated potential energy surface for the reaction of acetyl chloride on a $Ge_2Si_7H_{12}$ dimer cluster at the B3LYP/6-311++G(2df,pd) level of theory. To reach the [2+2] C═O cycloaddition and α-CH dissociation products, acetyl chloride passes through an oxygen dative-bonded state. A chlorine-bound minimum was also found between the vacuum level and the Cl dissociated product.

surface products and explain experimental trends, and we believe the $Ge_2Si_7H_{12}$ cluster provides an acceptable model for this purpose.

III. Theoretical Results and Discussion

Although several acyl halides were studied experimentally, we selected acetyl chloride as a representative compound with which to study different reaction pathways computationally. Figure 2 summarizes the reaction pathways investigated for the adsorption of acetyl chloride on a $Ge_2Si_7H_{12}$ dimer cluster. According to our calculations, formation of the [2+2] C═O cycloaddition and α-CH dissociation products requires passage through a weakly bound oxygen dative-bonded state located 3.3 kcal/mol below the energy of the reactants. The weak binding energy of the oxygen dative bond, approximately 9 kcal/mol less than that for acetone on $Ge_2Si_7H_{12}$,[28] is a result of the strong electronegative character of the chlorine atom. The weakly bound oxygen dative-bonded state also acts to push the barrier to formation of the [2+2] C═O cycloaddition and α-CH dissociation products to 5.9 and 7.6 kcal/mol above the entrance channel, respectively. Barriers of this magnitude in other organic/Ge(100)−2×1 systems[17,21] have been associated with inactive reaction pathways, and we believe that the probability of forming the [2+2] C═O cycloaddition or α-CH dissociation product for acetyl chloride on Ge(100)−2×1 is low.

In contrast, the Cl dissociation product likely forms through one of the following lower barrier pathways. The first pathway, illustrated in Figure 2, begins when the chlorine atom in acetyl chloride donates charge from the filled p orbitals in its valence shell to the electrophilic dimer atom of the surface to form a chlorine-bound precursor state. Acetyl chloride can then pass over a small barrier, 1.1 kcal/mol above the entrance channel, whereby the nucleophilic dimer atom donates its charge to the carbonyl carbon atom, thus abstracting the acetyl group, and ultimately forming the Cl dissociation product. The binding energy of the Cl dissociation product is in excess of 49 kcal/mol.

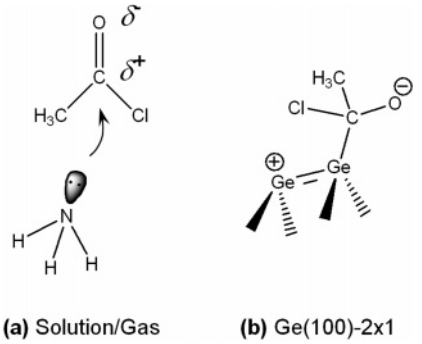

Figure 3. Comparison of (a) classic nucleophilic attack of the carbonyl carbon and an (b) analogous precursor state on the Ge(100)−2×1 dimer.

It is also conceivable that, rather than interact initially through the chlorine or oxygen atom, the nucleophilic Ge dimer atom could donate its electronic charge directly to the carbonyl carbon in a reaction analogous to the classic attack of the electron-deficient carbonyl carbon by a nucleophile (see Figure 3).[45] Hamers and co-workers provide evidence for this type of interaction in their study of trimethylamine and boron trifluoride coadsorption on Si(100)−2×1.[26] However, after placement of acetyl chloride in several initial orientations above the nucleophilic dimer atom in the calculations, we were unable to find a stable minimum for this state. If the chlorine atom was located near the electrophilic dimer atom, C−Cl dissociation always occurred as the calculation proceeded. Similar to the reaction of ethyl vinyl ketone on Ge(100)−2×1,[46] this suggests that there is little or no barrier to chlorine dissociation for this pathway.

While we cannot experimentally determine which Cl dissociation pathway actually occurs, the calculations show that the Cl dissociated product is the most kinetically and thermodynamically favored surface product by a significant margin. By making several assumptions, the branching ratios between the different products for acetyl chloride can be estimated. First, we assume that the transition from the precursor state to the final surface product is the rate-limiting step in this reaction and that there is a similar amount of surface accommodation in each precursor state. If we further assume that the preexponential factors are all identical, the branching ratios between the Cl dissociation product and the [2+2] C═O cycloaddition and α-CH dissociation products can be estimated as 3.0×10^3 and 5.5×10^4, respectively. On the basis of these single dimer cluster calculations, we expect the majority of the surface adducts to be the Cl dissociated product, formed with nearly 100% selectivity. Furthermore, the substantial margin of favorability for the Cl dissociation pathway of acetyl chloride suggests that similar C−X reactions (where X = Cl, Br) are highly likely for the other acyl halides as well. As will be discussed in the sections that follow, infrared and X-ray photoelectron data indicate that the C−X dissociation product is indeed the majority surface adduct, although a second surface species is also present.

IV. Experimental Results

Figure 4 is a compilation of the infrared absorption spectra obtained for acetyl chloride and acetyl bromide. More specifically, spectra a and b of Figure 4 are the spectra for a chemisorbed saturation exposure of acetyl chloride at 310 K and physisorbed multilayers at low temperature, respectively. Spectra c and d of Figure 4 are the spectra for a chemisorbed saturation exposure of acetyl bromide at 310 K and physisorbed multilayers at low temperature, respectively. As expected, the general features of the multilayer spectra for both compounds

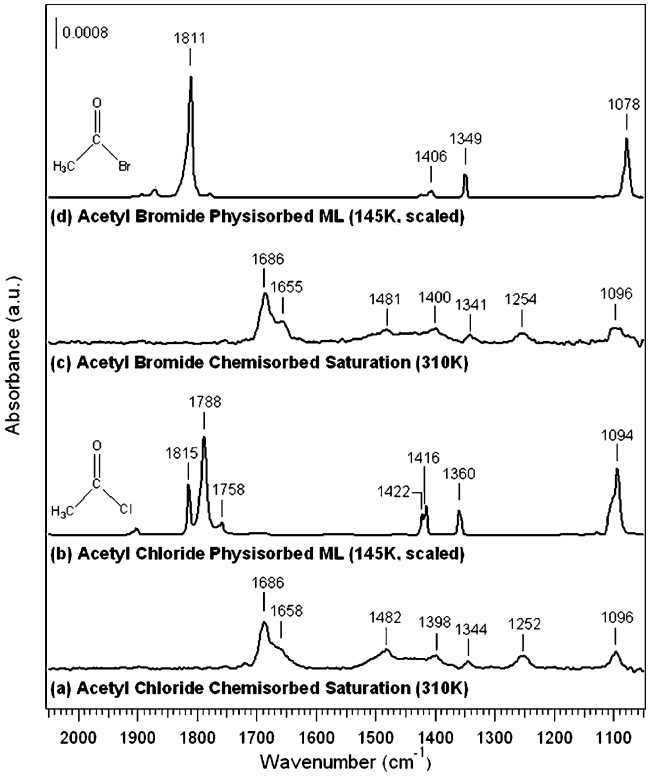

Figure 4. Infrared spectra of acetyl chloride and acetyl bromide on Ge(100)−2×1: (a) 0.2 L exposure of acetyl chloride at 310 K, (b) acetyl chloride multilayers at 145 K (scaled), (c) acetyl bromide saturation exposure at 310 K, and (d) acetyl bromide multilayers at 145 K (scaled).

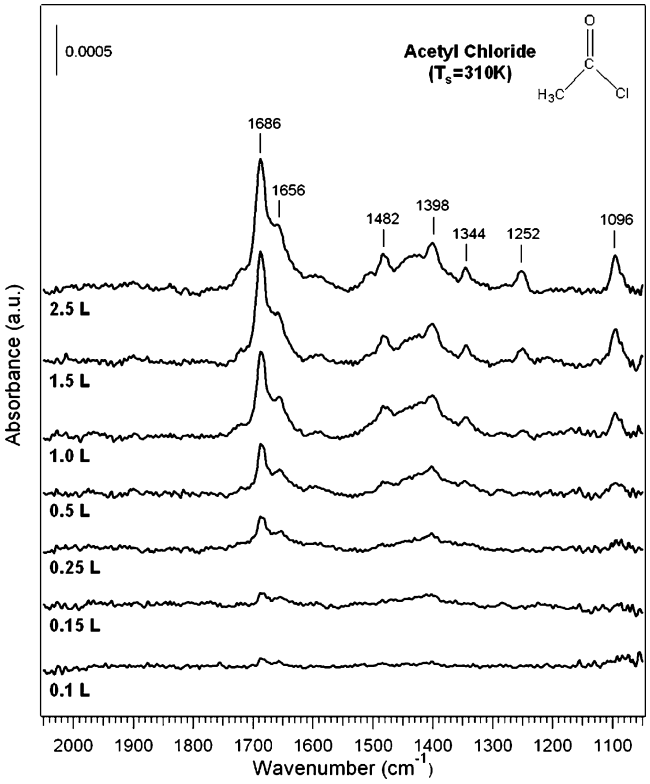

Figure 5. Coverage dependent infrared spectra of acetyl chloride on Ge(100)−2×1 at 310 K. Due to the low exposure required for saturation when using a directed doser, these spectra were recorded without a doser.

are similar. Absorption peaks at 1422/1416 and 1360 cm^{-1} for acetyl chloride and at 1406 and 1349 cm^{-1} for acetyl bromide are due to $\delta(CH_3)$ deformation modes. Modes at 1094 and 1078 cm^{-1} for acetyl chloride and acetyl bromide, respectively, can be attributed to a $\rho(CH_3)$ rocking mode.[47] However, the two compounds differ in the number of features present in the carbonyl stretching region near 1800 cm^{-1}. In the case of acetyl chloride (Figure 4b) several strong carbonyl stretching modes at 1815, 1788, and 1758 cm^{-1} are observed, while only a single peak at 1811 cm^{-1} is found for acetyl bromide, an observation that is consistent with the literature.[47−49] The type of splitting seen for acetyl chloride is attributed to the presence of different molecular conformers often observable for carbonyl-containing compounds in the solid phase and depends strongly on the experimental conditions.[50]

The location and intensity of the absorption modes in the 0.2 L saturation exposure spectrum of acetyl chloride on Ge(100)−2×1 at 310 K (Figure 4a) are nearly identical with those for acetyl bromide (Figure 4c). For the case of acetyl chloride, major infrared absorption peaks are observed at 1686, 1482, 1398, 1344, 1252, and 1096 cm^{-1}. The peaks in the acetyl bromide spectrum are shifted by no more than 3 cm^{-1} from the peaks in the acetyl chloride spectrum and are of similar intensity. The close resemblance of the chemisorbed spectra indicates that both molecules likely participate in the same surface reactions to create the same surface product distributions. A preliminary spectral analysis suggests the presence of a ν(C═O) stretching mode at 1686 cm^{-1}, which is red shifted over 100 cm^{-1} from its position in either multilayer, as well as various δ(C−H) bending modes below 1500 cm^{-1}. It is important to note that no ν(Ge−H) stretching modes, expected between 1980 and 1940 cm^{-1}, are present for either compound. Furthermore, the formation of Ge−Cl and Ge−Br surface bonds cannot be detected because their stretching frequency falls well below the 1100 cm^{-1} cutoff of the CaF_2 chamber windows. Figure 5 is a coverage dependent plot of acetyl chloride adsorbed at 310 K and shows that all vibrational modes grow in at similar rates.

To determine whether the absorption modes below 1500 cm^{-1} result from δ(C−H) bending or other vibrational modes, acetyl-d_3 chloride was examined. Spectra c and d of Figure 6 show the experimentally obtained infrared spectrum for a saturation exposure of acetyl-d_3 chloride at 310 K on Ge(100)−2×1 and corresponding multilayer spectrum at 145 K, respectively. For comparison, the chemisorbed and multilayer spectra of normal acetyl chloride are included in Figure 6, spectra a and b, respectively. The acetyl-d_3 chloride multilayer spectrum shows that, as expected, the methyl deformation and rocking modes significantly red shift to lower energies, and the only mode remaining visible above the infrared window cutoff is the $\delta(CD_3)$ symmetric deformation mode at 1126 cm^{-1}. Examination of the acetyl-d_3 chloride chemisorbed saturation spectrum shows that the strong absorption mode at 1686 cm^{-1} for the case of acetyl chloride (Figure 6a) red shifts only slightly and now appears at 1678 cm^{-1}. The peaks near 1398, 1344, and 1096 cm^{-1} present for chemisorbed acetyl chloride and acetyl bromide shift significantly upon deuteration of the acetyl group, confirming that they arise from various δ(C−H) deformation modes. On the other hand, the peaks at 1454 and 1265 cm^{-1} are not shifted significantly from those for acetyl chloride, and hence cannot be due to δ(C−D) modes. On the basis of the structure of acetyl chloride and the location of these absorbance bands, they likely correspond to some form of a C−O or C−C stretching mode, a topic that will be addressed in Section V.

Benzoyl chloride and pivaloyl chloride (more commonly known as trimethylacetyl chloride) do not contain potentially

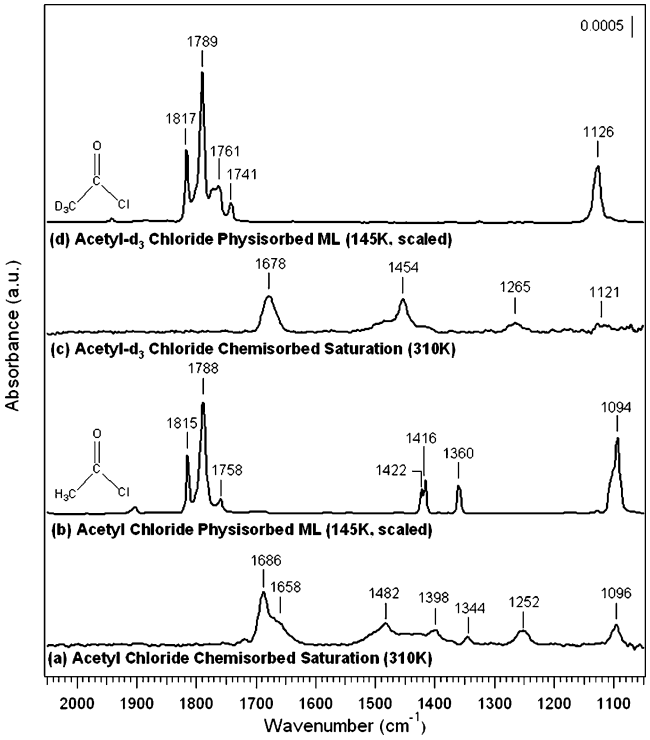

Figure 6. Infrared spectra of acetyl chloride and acetyl-d_3 chloride on Ge(100)−2×1: (a) 0.2 L exposure of acetyl chloride at 310 K, (b) acetyl chloride multilayers at 145 K (scaled), (c) acetyl-d_3 chloride saturation exposure at 310 K, and (d) acetyl-d_3 chloride multilayers at 145 K (scaled).

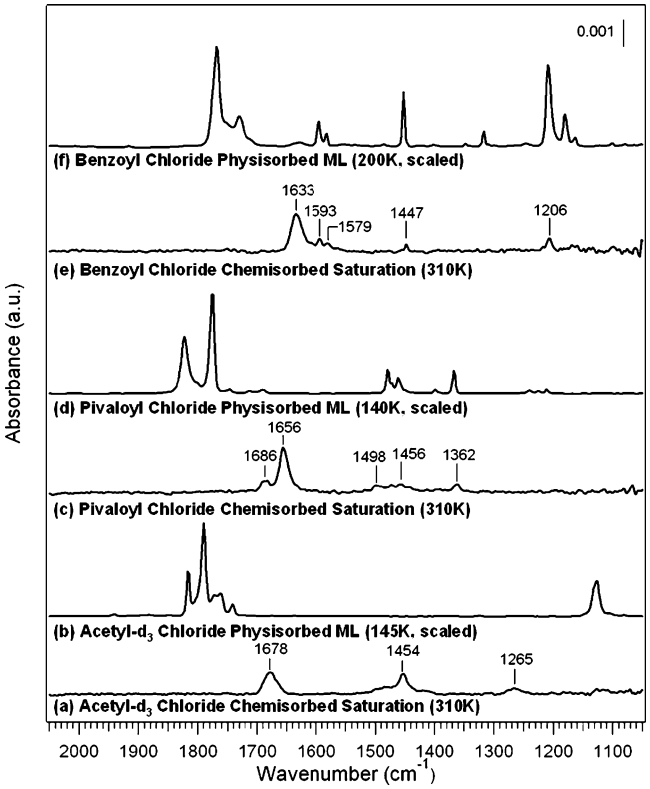

Figure 7. Infrared spectra of acetyl-d_3 chloride, pivaloyl chloride, and benzoyl chloride on Ge(100)−2×1: (a) saturation exposure of acetyl-d_3 chloride at 310 K, (b) acetyl-d_3 chloride multilayers at 145 K (scaled), (c) pivaloyl chloride saturation exposure at 310 K, (d) pivaloyl chloride multilayers at 140 K (scaled), (e) benzoyl chloride saturation exposure at 310 K, and (d) benzoyl chloride multilayers at 200 K (scaled).

reactive α-CH bonds and provide additional information regarding the reactivity of acyl halides toward Ge(100)−2×1. Figure 7 shows the chemisorbed saturation and low-temperature multilayer spectra for benzoyl chloride and pivaloyl chloride, as well as that for acetyl-d_3 chloride for comparison. The multilayer spectrum of benzoyl chloride in Figure 7f shows a carbonyl ν(C═O) stretching mode near 1770 cm^{-1} as well as a series of ring breathing modes at 1595, 1582, 1452, and 1209 cm^{-1}. Upon adsorption on Ge(100)−2×1 at room temperature, a strong vibration is observed at 1633 cm^{-1} in Figure 7e. While this mode has shifted appoximately 135 cm^{-1} from the position of the ν(C═O) stretch in the multilayer, the positions of peaks at 1593, 1579, 1447, and 1206 cm^{-1} are nearly identical with the ring modes in the multilayer, suggesting that an intact benzoyl group is present on the surface. Similarly, spectra c and d in Figure 7 show that the chemisorbed spectrum of pivaloyl chloride exhibits clear vibrational features at 1656/1686 cm^{-1} which are red shifted by over 120 cm^{-1} from the position of the ν(C═O) stretching mode in the multilayer. The δ(C−H) absorption peaks corresponding to the *tert*-butyl group of chemisorbed pivaloyl chloride at 1498, 1456, and 1362 cm^{-1} shift only slightly from their position in the multilayer, and are indicative of an intact pivaloyl group bound to the surface. No ν(Ge−H) modes are observed following adsorption of either compound.

Figure 8 displays the O(1s) and C(1s) photoelectron peaks for acetyl chloride and benzoyl chloride chemisorbed at saturation on Ge(100)−2×1 at room temperature. Although not shown, the Cl(2p) and Cl(2s) spectra indicate that Cl is present on the surface for both compounds. The O(1s) spectrum of acetyl chloride chemisorbed at saturation (Figure 8a) can be fit with two peaks centered at 531.5 and 532.9 eV. It is also possible to fit two peaks at 531.2 and 532.7 eV to the O(1s) spectrum of benzoyl chloride (Figure 8b). The integrated intensities of the O(1s) envelopes for acetyl chloride and benzoyl chloride are nearly identical, indicating similar surface coverages for both compounds. On the basis of the number of inflection points visible in the C(1s) spectra of acetyl chloride (Figure 8c), at least three chemical states exist, and we fit peaks at 284.0, 285.8, and 288.7 eV. For the case of benzoyl chloride (Figure 8d), we fit two peaks at 284.6 and 285.7 eV to the C(1s) envelope; no peak is observed near 288.7 eV. A comparison of the entire C(1s) peak area with that of pyridine, which has five carbons and is reported to saturate at 0.25 ML on Ge(100)−2×1,[51] enables us to determine that the surface coverages of acetyl chloride and benzoyl chloride are both near 0.5 ML (1 ML = one molecule per Ge surface atom).

V. Discussion

Two major conclusions can be drawn from the theoretical and experimental results presented above. First, a C−X dissociation reaction leads to the formation of surface-bound acyl groups on Ge(100)−2×1, and second, a percentage of the acetyl surface adducts appear to undergo an additional interaction with nearby surface atoms. We begin with a discussion of the C−X dissociation product. The spectral similarities for acetyl chloride and acetyl bromide adsorbed on Ge(100)−2×1 provide strong evidence that the C−X dissociation product, which retains the carbonyl functionality, is present on the surface for both compounds. Acyl halides are known to exhibit a substantially blue shifted ν(C═O) stretching frequency as compared to acetone, as a result of increased charge density in the carbonyl bond due to the neighboring halide atom.[52] For example, the ν(C═O) stretching modes of gas-phase acetyl fluoride, acetyl chloride, and acetyl bromide are reported to fall at 1869, 1822,

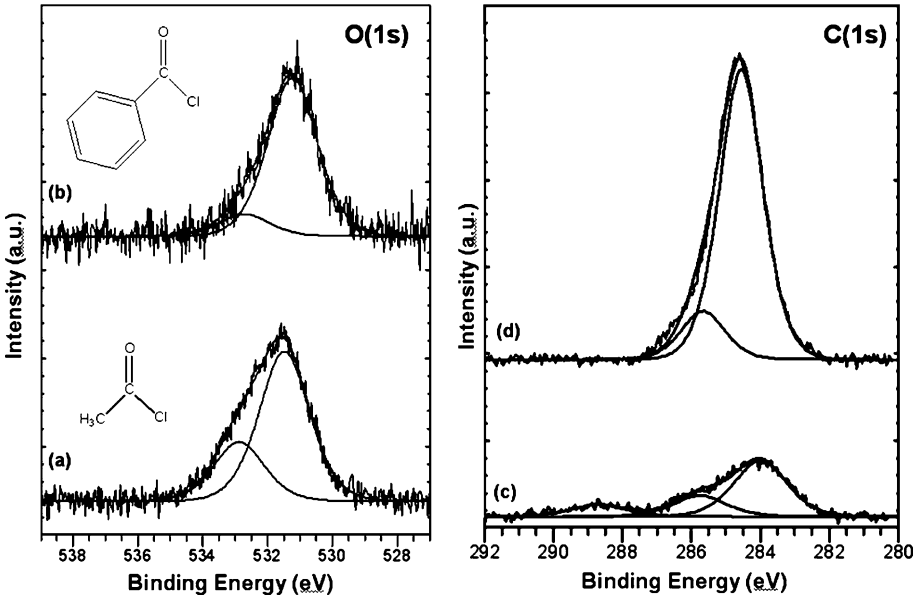

Figure 8. O(1s) and C(1s) X-ray photoelectron spectra of acetyl chloride and benzoyl chloride on Ge(100)−2×1 at room temperature: (a) O(1s) of acetyl chloride, (b) O(1s) of benzoyl chloride, (c) C(1s) of acetyl chloride, and (d) C(1s) of benzoyl chloride.

and 1821 cm^{-1}, respectively, while that of acetone is at 1736 cm^{-1}.[53] While clear differences are present in the ν(C═O) stretching region of the acetyl chloride and acetyl bromide multilayer spectra (Figure 4b,d), their chemisorption spectra are nearly identical (Figure 4a,c). This result indicates that upon chemisorption the halogen atom exerts a chemically insignificant influence on the acetyl group normal modes, and provides evidence that the halogen atom likely dissociates upon adsorption. We therefore believe the C−X dissociated product is the majority surface adduct following chemisorption of acetyl chloride and acetyl bromide, and assign the peak at 1686 cm^{-1} to the ν(C═O) stretching mode of a surface-bound acetyl moiety. At the same time, we cannot definitively assign the low energy shoulder near 1655 cm^{-1} for either acetyl chloride or acetyl bromide, although the presence of carbonyl bonds in slightly different surface environments is a likely explanation.

The chemisorption spectrum of acetyl-d_3 chloride on Ge(100)−2×1 (Figure 6c) is consistent with the presence of the C−X dissociation product. We assign the mode at 1678 cm^{-1} to the ν(C═O) stretch of the surface-bound acetyl-d_3 moiety based on its proximity to the same mode observed near 1685 cm^{-1} for the case of acetyl chloride and acetyl bromide. While no shoulder is visible for acetyl-d_3 chloride, the fwhm of the peak is large, which could be indicative of unresolved features from the acetyl group in multiple environments.

Since the large majority of aldehydes and ketones exhibit gas phase ν(C═O) stretching frequencies between 1700 and 1800 cm^{-1},[52] it is important to address the appearance of the surface-bound acetyl ν(C═O) stretching peak below 1700 cm^{-1}. After the reaction of an acetyl halide compound on Ge(100)−2×1 to form the C−X dissociated product, the halogen atom will be located at least two surface atoms away from the carbonyl functional group, as depicted in Figure 2. Due to the increased distance between the halide and carbonyl moiety in the surface species, the ν(C═O) stretching mode has significantly red shifted from its position in the multilayer toward that of acetone. However, the observed ν(C═O) stretching frequency of the C−X dissociated surface adduct, at 1686 cm^{-1}, is red shifted approximately 50 cm^{-1} *beyond* that of gaseous acetone[52] and we believe germanium−acetyl inductive interactions likely explain this observation. Similar to the case of nitriles,[17] the stretching frequency of carbonyl functional groups bonded directly to group IV atoms such as silicon and germanium can be red shifted from that of acetone by 30 cm^{-1}.[54] In their investigation of metal ketones, Bruns et al. report that the carbonyl bond is weakened by electron transfer from the π orbital of the C═O bond to the vacant d orbitals of the α-Ge atom.[54] This effect, in addition to the displacement of the halogen atom upon adsorption, provides substantial evidence for the appearance of the ν(C═O) stretching frequency near 1686 cm^{-1}. Furthermore, the large red shift of the ν(C═O) mode observed experimentally is consistent with our DFT calculations which indicate a 116 cm^{-1} shift upon adsorption of acetyl chloride in the Cl-dissociated state on a $Ge_2Si_7H_{12}$ dimer cluster.

The spectral differences observed between spectra a and c in Figure 6 further enable an assignment of the δ(C−H) deformation modes of the C−X dissociation product. The peaks present at 1398, 1344, and 1096 cm^{-1} for acetyl chloride are absent upon deuteration of the methyl group, and hence are assigned to various δ(C−H) modes. Since the acetyl functionality of both compounds is expected to remain intact following the C−X dissociation reaction, the multilayer methyl deformation modes should not shift significantly upon adsorption. Consistent with these expectations, the above deformation modes exhibit frequency shifts less than 25 cm^{-1} following adsorption for acetyl chloride and acetyl bromide (Figure 4). For example, the modes at 1416 and 1360 cm^{-1} in the acetyl chloride multilayer only shift to 1398 and 1344 cm^{-1}, respectively, following chemisorption. By comparison with the multilayer spectra (Figure 4b,d) we assign the peaks near 1400 and 1342 cm^{-1} in the chemisorbed monolayers of acetyl chloride and acetyl bromide to $\delta(CH_3)$ deformation modes, while the peak at 1096 cm^{-1} is assigned to a $\rho(CH_3)$ rocking mode.

The infrared spectra also rule out the existence of any significant quantity of the α-CH dissociation and [2+2] C═O cycloaddition adducts discussed in Section III. The strongest evidence against the α-CH dissociation product is the lack of a ν(Ge−H) stretching feature between 1980 and 1940 cm^{-1} for both acetyl chloride and acetyl bromide. Although the strong peak at 1686 cm^{-1} was assigned to the ν(C═O) stretching mode of the C−X dissociated product, it could result instead from the ν(C═C) stretching mode of the α-CH dissociation product.

In this case, the ν(C═C) mode of this product would be accompanied by a ν(Ge−H) stretching peak, but no such mode is observed between 1940 and 1980 cm^{-1}. Moreover, in the case of gas-phase Cl-, Br-, or I-substituted ethylenes, an increase in the mass of the halogen atom causes a red shift in the ν(C═C) stretching frequency,[55] as expected from the harmonic oscillator approximation. Since the α-CH dissociation product would consist of a halogen-substituted vinyl group attached to the surface, the ν(C═C) stretching frequency of the surface adducts resulting from adsorption of acetyl chloride and acetyl bromide would likely differ. However, no peak shifts are observed between the spectra of these compounds (Figure 4a,c), further supporting our assertion that the α-CH dissociation pathway does not proceed appreciably.

Existence of the [2+2] C═O cycloaddition product is more difficult to determine experimentally. ν(C−O) stretching modes in a strained environment, indicative of the four-membered ring of the [2+2] C═O cycloaddition product, were calculated to fall at 1025 cm^{-1}. This frequency falls below the infrared cutoff of CaF_2 and is thus difficult to observe with our experimental setup. However, the energetic results of the theoretical calculations help rule out this product. Should acetyl chloride or acetyl bromide surmount the relatively large predicted barrier to form the [2+2] C═O cycloaddition product, its surface lifetime is expected to be short. A first-order kinetic analysis with a preexponential factor of 10^{13} s^{-1}, believed to be a reasonable approximation for cycloaddition products on the related Si(100)−2×1 surface,[56] yields a surface lifetime on the order of microseconds at room temperature. This is extremely short when compared to the time scale of our spectroscopic measurements, which are on the order of 10^2 s. Therefore, the [2+2] C═O cycloaddition product is not expected to be observed.

We now turn to a discussion of the experimental evidence that supports an additional interaction between the acetyl adduct and the surface. The chemisorption spectra of acetyl chloride (Figure 6a) and acetyl-d_3 chloride (Figure 6c) indicate the presence of a surface species in addition to the simple C−X dissociation product. It is clear that the peaks at 1454 and 1265 cm^{-1} for acetyl-d_3 chloride are not shifted significantly from those for acetyl chloride, and hence cannot be due to C−H vibrational modes. On the basis of the types of bonds present in acetyl chloride and the location of these absorbance bands, these peaks likely correspond to some form of a C−O or C−C stretching mode. The frequency calculations of the C−X dissociation product indicate that the low energy mode near 1265 cm^{-1} is likely the ν(C−C) stretching vibration of the surface-bound acetyl group, a conclusion further supported by the ν(C−C) stretch of molecular acetone at 1216 cm^{-1}.[57] The assignment of the peak at 1454 cm^{-1} is less straightforward. Interestingly, this peak falls between that for a full carbonyl and that of a C−O single bond,[52] and could result from an extremely electron-deficient carbonyl bond.

In an attempt to further understand the molecular basis for the appearance of the unexpected feature at 1482 and 1454 cm^{-1} for acetyl chloride and acetyl-d_3 chloride, respectively, spectra of adsorbed benzoyl chloride and pivaloyl chloride were also examined. The infrared spectra shown in Figure 7 are consistent with a Cl dissociation product for both benzoyl chloride and pivaloyl chloride. Similar to the case of the acetyl halides, no ν(Ge−H) modes are visible in Figure 7c,e, indicating that no hydrogen-dissocation reactions take place at 310 K. The ring breathing and *tert*-butyl δ(C−H) modes below 1600 cm^{-1} for benzoyl chloride and pivaloyl chloride, respectively, are similar to their respective multilayers. Analogous to the reaction of the acetyl halides, these spectral similarities suggest that the benzoyl and pivaloyl groups are intact following adsorption. The observed red shift of the ν(C═O) peak from its position in the multilayer for both compounds is due to dissociation of the halide atom as well as a germanium−acyl inductive effect discussed earlier for the acetyl halides. Furthermore, the ν(C═O) peak resulting from the C−X dissociation of benzoyl chloride is red shifted approximately 50 cm^{-1} from that of adsorbed acetyl chloride, which we attribute to electron delocalization between the carbonyl and benzene ring of the surface-bound benzoyl group.[52] Interestingly, neither benzoyl chloride nor pivaloyl chloride appear to form the intense, anomalous mode near 1450 cm^{-1}. Besides the ring breathing mode observed at 1447 cm^{-1} for chemisorbed benzoyl chloride and the weak *tert*-butyl δ(C−H) modes between 1498 and 1456 cm^{-1} for chemisorbed pivaloyl chloride, no strong absorption modes similar to those for the acetyl halides are visible between 1400 and 1500 cm^{-1}. This suggests that the benzene ring or *tert*-butyl substituent group inhibits the surface interaction leading to the unexpected vibrational mode seen for acetyl halides adsorbed on Ge(100)−2×1.

We now turn to our X-ray photoelectron spectra to determine the source of these unexpected vibrational modes. We begin by assigning each photoelectron peak component and continue with a discussion of the unexpected surface species. The largest component of the acetyl chloride and benzoyl chloride O(1s) spectra falls at 531.5 and 531.2 eV, respectively (Figure 8a,b). Since the carbonyl O(1s) peak of a polycarbonate thin film appears at 532.4 eV,[58] and the Pauling electronegativity difference between that of germanium (2.01) and carbon (2.55) is expected to increase the electron density of the carbonyl bond, we attribute these low binding energy peaks to the carbonyl oxygen of the surface-bound acetyl group of the C−X dissociation product. In addition, the higher intensity of the low binding energy O(1s) peaks is consistent with the C−X dissociation adduct as the majority product as deduced from the infrared spectra. The weaker, high binding energy component at 532.9 and 532.7 eV for acetyl chloride and benzoyl chloride, respectively, indicates that an electron deficient oxygen atom is present at the surface.

We fit two peaks at 284.6 and 285.7 eV in the C(1s) photoelectron spectrum of benzoyl chloride (Figure 8d), and assign these to the benzene ring carbons and carbonyl carbon of a surface-bound benzoyl group, respectively. The location of the benzene ring photoelectron peak at 284.6 eV is consistent with that of polycarbonate[58] as well as 9,10-phenanthrenequinone adsorbed on Si(100)−2×1.[59] In agreement with the expected benzene-to-carbonyl carbon ratio for the surface-bound benzoyl moiety of the C−X dissociation product, the area ratio of the low to high binding energy peaks is approximately 6:1.

The C(1s) photoelectron spectrum of acetyl chloride is more complex than that of benzoyl cloride. Since methyl and carbonyl carbons fall near 285.0 and 287.6 eV, respectively,[58] and the electronegativity difference between carbon and germanium is expected to transfer charge from the surface to the carbonyl bond, we assign the peaks at 284.0 and 285.8 eV to the methyl and carbonyl carbon of the surface-bound acetyl group, respectively. Similar binding energy shifts are reported for the Si−C bond in cyclopentene adsorbed on Si(100)−2×1 at room temperature.[60] The weak peak component located at 288.7 eV (Figure 8c) for acetyl chloride is assigned to an electron deficient carbon atom, and we believe it results from the same surface species that leads to the high binding energy O(1s) peak at 532.9 eV.

It is clear that the C(1s) component peaks at 284.0 and 285.8 eV are not the same area, as would be expected stoichiometrically in a C−X dissociation product. In addition, the two distinct carbon atoms of acetyl chloride suggest that an even number of peak components should be present. However, only three components are fit to the C(1s) spectrum of acetyl chloride based on the observed number of inflection points. Due to this discrepancy, we postulate that the additional area of the 284.0 eV peak is potentially due to an unresolveable carbon component from the species responsible for the high binding energy C(1s) peak at 288.7 eV.

The high binding energy C(1s) and O(1s) photoelectron peaks observed for acetyl chloride adsorbed on Ge(100)−2×1 are evidence of a second product or surface interaction. In the case of benzoyl chloride, no high binding energy C(1s) peaks are present, and the O(1s) component of benzoyl chloride at 532.7 eV is nearly three times weaker than that of acetyl chloride. It is important to note that although a weak high binding energy component still appears to be present in the benzoyl chloride O(1s) spectrum, this is potentially an artifact of using strictly Voigt line shapes which do not take into account the inherent asymmetries of X-ray photoelectron spectra previously reported in other organic/semiconductor systems.[61,62] Since benzoyl chloride exhibits neither the high binding energy photoelectron peak near 532.9 eV nor the intense, red shifted ν(C═O) stretching mode observed near 1480 cm^{-1} for acetyl chloride, we can infer that these two spectral features result from the same surface species or interaction.

We postulate that this second species observed for the acetyl halides by both infrared and X-ray photoelectron studies involves an oxygen-donation interaction. In certain classes of organometallic compounds, known as metal carbonyls, electrons from the carbonyl π system or from one of its lone pairs can be donated to different metal centers, and this type of "bridging" donation leads to substantial red shifts of the ν(C═O) stretching frequency.[63] If acetyl halides form a halogen-dissociation product next to a vacant dimer, the potential exists for the oxygen of the acetyl moiety to donate electronic charge from one of its lone pairs to the electrophilic atom of a neighboring surface dimer. Such an interaction occurring across a trench is illustrated in Figure 9. Following this type of interaction, the carbonyl moiety would be substantially weakened due to the electron transfer from the carbonyl bond to the surface, and cause an increase in the binding energy for the O(1s) and C(1s) photoelectrons resulting from the carbonyl bond. A similar binding energy shift is reported for the electron-deficient nitrogen and carbon atoms of trimethylamine and ethylenediamine following adsorption in the dative-bonded state on Si(100)−2×1[64] and Ge(100)−2×1,[35] respectively. In addition, loss of electron density would lead to a red shift of the ν(C═O) stretching mode of the C−X dissociation product, consistent with the strong peaks near 1450 cm^{-1} for the acetyl halides. Together these data suggest that a percentage of the surface-bound acetyl groups of the C−X dissociated product are donating charge to nearby surface atoms.

Although Figure 9 illustrates charge donation within the context of a vacant neighboring dimer, the near 0.5 ML coverage for acetyl chloride (i.e., one molecule per surface dimer) indicates that an interaction with already reacted surface dimers may be possible as well. This conclusion is further supported by the lack of coverage dependent adsorption behavior for acetyl chloride. If charge donation could occur only with a vacant dimer, a strong coverage dependence would be expected, with a significantly larger percentage of surface species donating

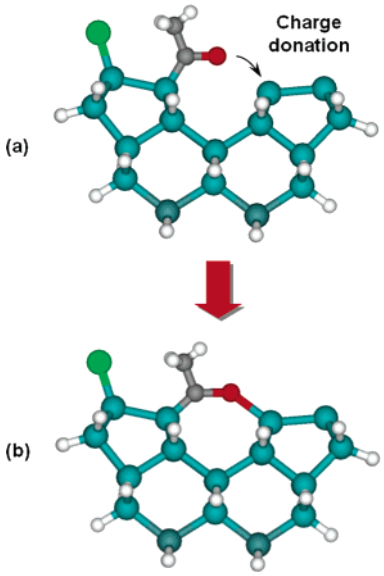

Figure 9. Trench dimer cluster model illustrating a possible charge donation mechanism for acetyl chloride on Ge(100)−2×1: (a) the Cl dissociation product adjacent to a vacant surface dimer and (b) the oxygen of the acetyl group donating charge to a neighboring surface atom. In the model, Cl is represented by green, O by red, H by white, and C by grey.

charge at low coverages. However, as shown in Figure 5, the coverage-dependent infrared spectra of acetyl chloride on Ge(100)−2×1 do not reveal a significant shift in the product distribution as coverage is increased. A coverage dependent study of acetyl-d_3 chloride (not shown) reveals similar behavior. The minimal spectral change observed with increasing coverage, as well as the high absolute coverage, leads us to postulate that a charge donation interaction does not necessarily require a vacant surface dimer. As discussed above, metal atoms can form multiple bonds with carbonyl groups and we speculate that this type of interaction may be possible on Ge(100). Furthermore, since halide atoms are known to roughen Si(100)−2×1,[65,66] their presence may lead to surface bond cleavage that would provide another route for an oxygen−surface interaction.

The reactivity of benzoyl chloride and pivaloyl chloride, which do not appear to undergo the same charge donation observed for the acetyl halides, must be addressed. The pivaloyl group is large sterically when compared to the methyl group of acetyl chloride, while the benzoyl group is both sterically large and electronically distinct. The steric similarities of both groups suggest that sterics play an important role in the apparent prevention of adsorbate−surface charge donation for pivaloyl chloride and benzoyl chloride. We speculate that this influence is likely manifest as an interaction between the *tert*-butyl group or benzene ring of the surface product, and the surface or a neighboring adsorbate. The C−C═O bond of the acyl moiety is positioned parallel to the dimer rows in the C−X dissociation transition state, as shown in Figure 10. On the basis of this geometry, surface-bound acetyl, pivaloyl, or benzoyl groups would need to rotate along the Ge−C bond axis to form the structure illustrated in Figure 9. In the case of the acetyl halides, where minimal steric interactions between the methyl group and the surface hinder rotation, an interaction is possible. However, for pivaloyl and benzoyl chloride, steric interactions may be sufficiently large such that rotation and formation of this interaction is prevented. Scanning tunneling microscopy experiments or multiple-dimer cluster calculations would allow the adsorbate−surface charge donation postulated in the present work to be verified.

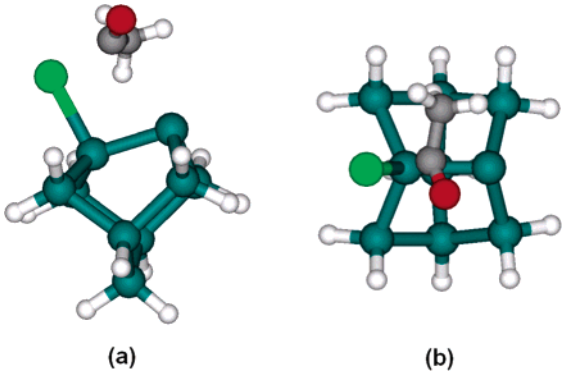

Figure 10. (a) Side and (b) top view of the Cl-dissociation transition state calculated on a $Ge_2Si_7H_{12}$ dimer cluster.

VI. Conclusion

The reaction of a series of acyl halides on Ge(100)−2×1 has been investigated with MIR-IR spectroscopy, XPS, and DFT calculations. The majority product, as predicted by DFT calculations, is the C−X dissociation product. However, a more complex product distribution is observed for the acetyl halides studied. Infrared absorption features between 1480 and 1450 cm^{-1} as well as high binding energy photoelectron peaks likely result from an interaction where the lone pair of the surface-bound acetyl functionality donates charge to a neighboring surface atom. Benzoyl chloride and pivaloyl chloride are not found to undergo charge donation. Interactions between the surface and sterically bulky benzene and *tert*-butyl substituent groups are proposed to explain this observation.

The fact that the carbonyl moiety can be retained upon adsorption could provide another avenue to the subsequent layer-by-layer deposition of ultrathin films. Several different reaction schemes can be envisioned. Most simply, the acetyl moiety of the C−X dissociated product could react with a strong nucleophile such as ammonia to form an imine which could then be further derivatized. Additionally, hydrogen atoms could be used to directly form an alcohol from the surface-bound acyl groups which could then react with other acyl halides to form various esters. This process would be similar to atomic layer deposition of high-κ dielectrics but exploit the tailorability inherent in organic materials to provide customized properties for a specific application.

Acknowledgment. This work was supported by the National Science Foundation (CHE 0245260). M.A.F. would like to acknowledge the National Science Foundation for financial support in the form of a Graduate Research Fellowship. A.J.K. acknowledges support from the Stanford President's Scholar Program and the Merck Award for Student Research. D.W.P. thanks Stanford University for support in the form of a Stanford Graduate Fellowship. Experimental assistance from Rebecca Gerard, Yvonne Edmonds, and Ansoon Kim and scientific discussions with James A. Van Deventer and Charles B. Musgrave were greatly appreciated.

Supporting Information Available: Complete ref 38. This material is available free of charge via the Internet at http://pubs.acs.org.

References and Notes

(1) Lopinski, G. P.; Wayner, D. D. M.; Wolkow, R. A. *Nature* **2000**, *406*, 48.
(2) Hurley, P.; Ribbe, A.; Buriak, J. *J. Am. Chem. Soc.* **2003**, *125*, 11334.
(3) Guisinger, N.; Basu, R.; Baluch, A.; Hersam, M. *Ann. N.Y. Acad. Sci.* **2003**, *1006*, 227.
(4) Guisinger, N. P.; Greene, M. E.; Basu, R.; Baluch, A. S.; Hersam, M. C. *Nano Lett.* **2004**, *4*, 55.
(5) Strother, T.; Knickerbocker, T.; Russell, J. N.; Butler, J. E.; Smith, L. M.; Hamers, R. J. *Langmuir* **2002**, *18*, 968.
(6) Wolkow, R. A. *Annu. Rev. Phys. Chem.* **1999**, *50*, 413.
(7) Hamers, R. J.; Coulter, S. K.; Ellison, M. D.; Hovis, J. S.; Padowitz, D. F.; Schwartz, M. P.; Greenlief, C. M.; Russell, J. N. *Acc. Chem. Res.* **2000**, *33*, 617.
(8) Bent, S. F. *Surf. Sci.* **2002**, *500*, 879.
(9) Lu, X.; Lin, M. C. *Int. Rev. Phys. Chem.* **2002**, *21*, 137.
(10) Filler, M. A.; Bent, S. F. *Prog. Surf. Sci.* **2003**, *73*, 1.
(11) Buriak, J. M. *Chem. Rev.* **2002**, *102*, 1271.
(12) Sieval, A. B.; Linke, R.; Heij, G.; Meijer, G.; Zuilhof, H.; Sudholter, E. J. R. *Langmuir* **2001**, *17*, 7554.
(13) Lees, I. N.; Lin, H. H.; Canaria, C. A.; Gurtner, C.; Sailor, M. J.; Miskelly, G. M. *Langmuir* **2003**, *19*, 9812.
(14) Voicu, R.; Boukherroub, R.; Bartzoka, V.; Ward, T.; Wojtyk, J. T. C.; Wayner, D. D. M. *Langmuir* **2004**, *20*, 11713.
(15) De Smet, L. C.; Pukin, A. V.; Sun, Q.-Y.; Eves, B. J.; Lopinski, G. P.; Visser, G. M.; Zuilhof, H.; Sudholter, E. J. *Appl. Surf. Sci.* **2005**, *252*, 24.
(16) Wang, G. T.; Mui, C.; Tannaci, J. F.; Filler, M. A.; Musgrave, C. B.; Bent, S. F. *J. Phys. Chem. B* **2003**, *107*, 4982.
(17) Filler, M. A.; Mui, C.; Musgrave, C. B.; Bent, S. F. *J. Am. Chem. Soc.* **2003**, *125*, 4928.
(18) Bournel, F.; Gallet, J.; Kubsky, S.; Dufour, G.; Rochet, F.; Simeoni, M.; Sirotti, F. *Surf. Sci.* **2002**, *513*, 37.
(19) Teague, L. C.; Boland, J. J. *J. Phys. Chem. B* **2003**, *107*, 3820.
(20) Barriocanal, J. A.; Doren, D. J. *J. Am. Chem. Soc.* **2001**, *123*, 7340.
(21) Mui, C.; Han, J. H.; Wang, G. T.; Musgrave, C. B.; Bent, S. F. *J. Am. Chem. Soc.* **2002**, *124*, 4027.
(22) Bitzer, T.; Richardson, N. V. *Appl. Surf. Sci.* **1999**, *145*, 339.
(23) Kim, A.; Filler, M. A.; Kim, S.; Bent, S. F. *J. Am. Chem. Soc.* **2005**, *127*, 6123.
(24) Ritala, M.; Leskela, M. *Handbook of Thin Film Materials*; Academic Press: San Diego, CA, 2002.
(25) Carey, F. A.; Sundberg, R. J. *Advanced Organic Chemistry*, 4th ed.; Plenum Press: New York, 2001.
(26) Cao, X. P.; Hamers, R. J. *J. Phys. Chem. B* **2002**, *106*, 1840.
(27) Armstrong, J. L.; White, J. M.; Langell, M. *J. Vac. Sci. Technol. A* **1997**, *15*, 1146.
(28) Wang, G. T.; Mui, C.; Musgrave, C. B.; Bent, S. F. *J. Phys. Chem. B* **2001**, *105*, 12559.
(29) Eng, J.; Raghavachari, K.; Struck, L. M.; Chabal, Y. J.; Bent, B. E.; Flynn, G. W.; Christman, S. B.; Chaban, E. E.; Williams, G. P.; Radermacher, K.; Manti, S. *J. Chem. Phys.* **1997**, *106*, 9889.
(30) Hovis, J. S.; Liu, H.; Hamers, R. J. *Appl. Phys. A* **1998**, *66*, S553.
(31) Kim, A.; Choi, D. S.; Lee, J. Y.; Kim, S. *J. Phys. Chem. B* **2004**, *108*, 3256.
(32) Hofer, W. A.; Fisher, A. J.; Bitzer, T.; Rada, T.; Richardson, N. V. *Chem. Phys. Lett.* **2002**, *355*, 347.
(33) Lee, J. Y.; Jung, S. J.; Hong, S.; Kim, S. *J. Phys. Chem. B* **2005**, *109*, 348.
(34) Rangan, S.; Kubsky, S.; Gallet, J. J.; Bournel, F.; Le Guen, K.; Dufour, G.; Rochet, F.; Funke, R.; Kneppe, M.; Piaszenski, G.; Kohler, U.; Sirotti, F. *Phys. Rev. B* **2005**, *71*, 125320.
(35) Kim, A.; Filler, M. A.; Kim, S.; Bent, S. F. *J. Phys. Chem. B* **2005**, *109*, 19817.
(36) Zandvliet, H. J. W. *Phys. Rep.* **2003**, *388*, 1.
(37) Shirley, D. A. *Phys. Rev. B* **1972**, *5*, 4709.
(38) Frisch, M. J.; et al. *Gaussian 98*, Revision A.5; Gaussian, Inc.: Pittsburgh, PA, 1998.
(39) Kohn, W.; Sham, L. J. *Phys. Rev.* **1965**, *140*, A1133.
(40) Lee, C. T.; Yang, W. T.; Parr, R. G. *Phys. Rev. B* **1988**, *37*, 785.
(41) Vosko, S. H.; Wilk, L.; Nusair, M. *Can. J. Phys.* **1980**, *58*, 1200.
(42) Becke, A. D. *J. Chem. Phys.* **1993**, *98*, 5648.
(43) Weldon, M. K.; Queeney, K. T.; Chabal, Y. J.; Stefanov, B. B.; Raghavachari, K. *J. Vac. Sci. Technol. B* **1999**, *17*, 1795.
(44) Mui, C.; Bent, S. F.; Musgrave, C. B. *J. Phys. Chem. A* **2000**, *104*, 2457.
(45) McMurry, J. *Organic Chemistry*, 5th ed.; Brooks/Cole Pub Co: Pacific Grove, CA, 1999.
(46) Wang, G. T.; Mui, C.; Musgrave, C. B.; Bent, S. F. *J. Am. Chem. Soc.* **2002**, *124*, 8990.
(47) Durig, J.; Davis, J.; Guirgis, G. *J. Raman Spectrosc.* **1994**, *25*, 189.
(48) Kogure, N.; Hatakeyama, R.; Suzuki, E.; Watari, F. *J. Mol. Struct.* **1993**, *299*, 105.
(49) Kogure, N.; Ono, T.; Suzuki, E.; Watari, F. *J. Mol. Struct.* **1993**, *296*, 1.

(50) Coleman, W. M., III; Gordon, B. M. *Appl. Spectrosc.* **1987**, *41*, 1169.
(51) Hong, S.; Cho, Y. E.; Maeng, J. Y.; Kim, S. *J. Phys. Chem. B* **2004**, *108*, 15229.
(52) Lambert, J. B.; Shurvell, H. F.; Lightner, D. A.; Cooks, R. G. *Organic Structural Spectroscopy*; Prentice Hall: Upper Saddle River, NJ, 1998.
(53) Overend, J.; Scherer, J. R. *Spectrochim. Acta* **1960**, *16*, 773.
(54) Bruns, R.; Kuznesof, P. *J. Organomet. Chem.* **1973**, *56*, 131.
(55) Bellamy, L. J. *The Infrared Spectra of Complex Molecules*, 2nd ed.; Chapman and Hall: London, UK, 1980.
(56) Wang, Z.; Seebauer, E. G. *Appl. Surf. Sci.* **2001**, *181*, 111.
(57) Shimanouchi, T. *Tables of Molecular Vibrational Frequencies*; National Bureau of Standards: Washington, DC, 1972.
(58) Patnaik, A.; Li, C. L. *J. Appl. Phys.* **1998**, *83*, 3049.
(59) Fang, L. A.; Liu, J. M.; Coulter, S.; Cao, X. P.; Schwartz, M. P.; Hacker, C.; Hamers, R. J. *Surf. Sci.* **2002**, *514*, 362.
(60) Liu, H. B.; Hamers, R. J. *Surf. Sci.* **1998**, *416*, 354.
(61) Rochet, F.; Bournel, F.; Gallet, J. J.; Dufour, G.; Lozzi, L.; Sirotti, F. *J. Phys. Chem. B* **2002**, *106*, 4967.
(62) Yeom, H. W.; Baek, S. Y.; Kim, J. W.; Lee, H. S.; Koh, H. *Phys. Rev. B* **2002**, *66*, 115308.
(63) Pruchnik, F. P. *Organometallic Chemistry of the Transition Elements*; Plenum Press: New York, 1990.
(64) Cao, X. P.; Hamers, R. J. *J. Am. Chem. Soc.* **2001**, *123*, 10988.
(65) Herrmann, C. F.; Chen, D. X.; Boland, J. J. *Phys. Rev. Lett.* **2002**, *89*, 096102.
(66) Xu, G. J.; Graugnard, E.; Petrova, V.; Nakayama, K. S.; Weaver, J. H. *Phys. Rev. B* **2003**, *67*, 125320.